

## Time-resolved photoluminescence study of hydrogenated amorphous silicon nitride

Kwang Soo Seol

*RIKEN (The Institute of Physical and Chemical Research), 2-1 Hirosawa, Wako-shi, Saitama 351-0198, Japan*

Takashi Watanabe, Makoto Fujimaki, Hiromitsu Kato, and Yoshimichi Ohki\*

*Department of Electrical, Electronics, and Computer Engineering, Waseda University, 3-4-1 Ohkubo, Shinjuku-ku, Tokyo 169-8555, Japan*

Makoto Takiyama

*NSC Electron Corp., 3434 Shimada, Hikari-shi, Yamaguchi 743-0063, Japan*

(Received 20 September 1999; revised manuscript received 24 January 2000)

Time-resolved measurements of photoluminescence were carried out on a hydrogenated amorphous silicon nitride film prepared by low-pressure chemical vapor deposition. When excited with 5.0-eV photons, photoluminescence occurs over a broad spectrum ranging from 1.8 to 3.6 eV. The peak energy of this photoluminescence varies with time from several nanoseconds to nearly 1 ms. These results are explained by a combination of an excitonlike recombination process and a radiative tunneling recombination process of photogenerated carriers within the band-tail states, which are affected by the contributions of thermalization, the Coulombic interaction, and the extent of localization.

Near-stoichiometric hydrogenated amorphous silicon nitride ( $a\text{-SiN}_x\text{:H}$ ,  $x \approx 1.33$ ) is one of the most important dielectric materials in microelectronics fabrication. This material is used as a gate insulator in field-effect or thin-film transistors, as a charge storage layer in nonvolatile memories, or as a capacitor dielectric in dynamic random access memories. It is well established that the localized states in the band gap or at the band tails in this material affect device performance.<sup>1-4</sup> Much work has been carried out on this subject. Electrical measurements and electron spin resonance (ESR) studies have revealed that two paramagnetic defects known as the *K* center<sup>1-3</sup> ( $\text{N}_3 \equiv \text{Si} \cdot$ , where  $\equiv$  and  $\cdot$  denote three separate bonds and an unpaired electron, respectively) and the *N* center<sup>2-4</sup> ( $\text{Si}_2 = \text{N} \cdot$ , where  $=$  denotes two separate bonds) are the key charge centers in  $a\text{-SiN}_x\text{:H}$ .

Photoluminescence (PL), a powerful tool for the study of localized states, has been used on this material, and several PL bands between 1.8 and 4.0 eV have been reported in near-stoichiometric, silicon-rich, or nitrogen-rich  $a\text{-SiN}_x\text{:H}$ .<sup>5-9</sup> Among these PL bands a broad PL band centered around 2.5 eV has been widely reported for near-stoichiometric or nitrogen-rich  $a\text{-SiN}_x\text{:H}$ .<sup>5-9</sup> We have recently reported that this PL has very similar properties to the PL observed in hydrogenated amorphous silicon ( $a\text{-Si:H}$ ).<sup>5</sup> This fact suggests that the origin of this PL may be similar to that of  $a\text{-Si:H}$ . However, the information on this PL band is still not sufficient to understand the mechanism. In this report, we discuss this mechanism based on the results of time-resolved PL measurements on  $a\text{-SiN}_x\text{:H}$  performed over the time scale from nanoseconds to milliseconds.

The  $a\text{-SiN}_x\text{:H}$  samples used in this study were deposited on a *p*-type (100) silicon substrate by low-pressure chemical vapor deposition with a mixture of dichlorosilane ( $\text{Si}_2\text{H}_2\text{Cl}_2$ ) and ammonia ( $\text{NH}_3$ ) gases at a pressure of 65 Pa and at 650 or 750 °C. A detailed description of the samples used in this study is listed in Table I. The hydrogen content and the atomic ratio of N/Si (for Table I) were measured by Ruther-

ford backscattering, and the dielectric constant was measured by the capacitance-voltage method at 1 MHz. The thickness of each sample, as measured by ellipsometry, was 75 nm.

Time-resolved PL spectra were measured at room temperature using a monochromator equipped with an intensified charge-coupled device (ICCD) array. The ICCD array was gated by a pulse generator connected to a delay circuit, and the delay time between the laser pulse and the gate pulse was monitored with an oscilloscope. The gate pulse width or the PL observation time was adjusted from 50 ns to 4  $\mu\text{s}$  so that clear PL spectra could be obtained. Due to the substantial widths of the excimer laser and the gate pulse, this system is not suitable for decays on the order of a nanosecond. For this purpose, the PL decay was measured at 20 K using a single-photon counting technique excited by synchrotron radiation (SR) operated in a single-bunch mode (the time interval of SR pulses is 177.6 ns; the apparent pulse width is 550 ps) at the BL 1B line of the UVSOR (ultraviolet synchrotron orbital radiation) facility (Institute for Molecular Science, Okazaki, Japan).

Figure 1 shows typical time-resolved PL spectra measured in sample A. Curve (a) is the spectrum obtained by measuring over the whole PL time region of 0.1 s without

TABLE I. Samples.

Sample	Dielectric constant	Atomic ratio N/Si	H content (mol %)
A	4.7	1.24	3.93
B	5.2	1.54	6.05
C	6.0	1.57	5.43
D	6.1	1.36	4.01
E	6.2		
F	6.3	1.44	4.00
G	6.3	1.43	3.84

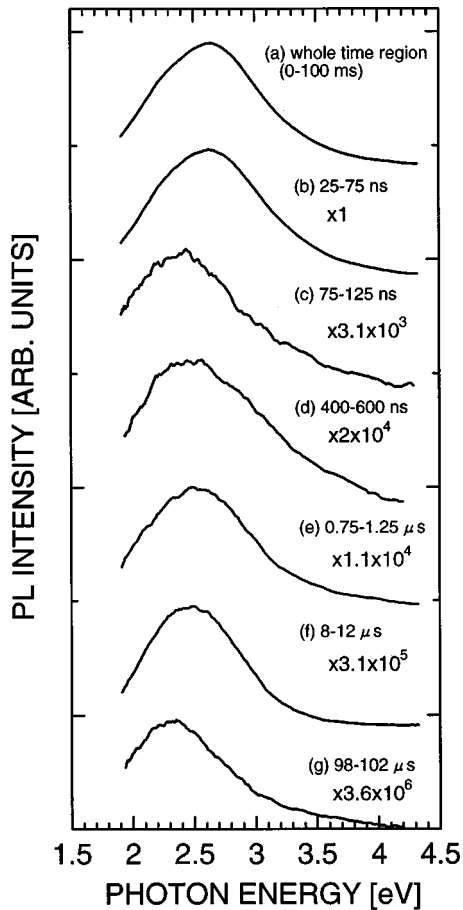


FIG. 1. Typical time-resolved PL spectra of sample A excited by 5.0-eV photons from the KrF excimer laser. The numerals following (a)–(g) indicate the observed time regions.

any delay. A Gaussian-shaped broad PL band, which is very similar to the PL's observed in near-stoichiometric  $a\text{-SiN}_x\text{:H}$ ,<sup>5–9</sup> was observed. The curves (b)–(g) correspond to the spectra measured at given time intervals after KrF excimer laser excitation. A shift of the PL peak as a function of the delay time was observed, i.e., first to red, then to blue, and then back to red again. Similar phenomena were observed in all the samples tested. Figure 2 shows the details of the shift observed in samples A, B, and F. The ordinate in Fig. 2 is the difference between the peak position of the different spectra, measured at various delay times, and the peak position of the time-integrated spectrum, e.g., curve (a) of Fig. 1. The horizontal bar at each data point shows the time interval used for the spectrum measurement. Furthermore, the vertical bar whose height is equal to the full width of the three-hundredth maximum of the spectrum is shown in order to provide a measure of the error in determining the peak energy. The redshifts at the initial and the final stages are common to all the samples, but the blueshift, after a delay of  $\sim 100$  ns, is not apparent in sample F.

Similar time-resolved PL measurements have been carried out by several authors on  $a\text{-Si:H}$  and its alloys<sup>10–17</sup> with oxygen ( $a\text{-SiO}_x\text{:H}$ ) and carbon ( $a\text{-SiC}_x\text{:H}$ ) and reveal various patterns in the PL peak shifts for these materials. However, it is widely accepted that three different effects, namely, thermalization, the Coulombic interaction, and the energy distribution of localized states, influence the recom-

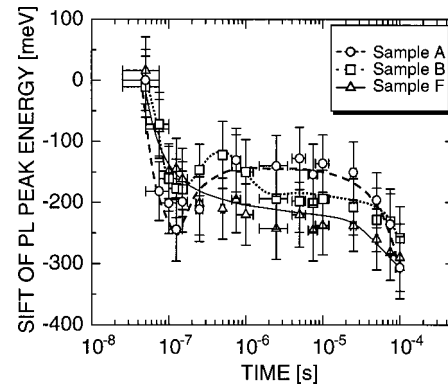


FIG. 2. The shifts of the PL peak position as a function of time after excitation for samples A, B, and F. The shift was obtained by subtracting the peak energy of the time-integrated spectrum, e.g., (a) of Fig. 1, from those of spectra measured at various delay times. The horizontal and vertical bars on the data points indicate the time interval used for the spectrum measurement and the full width of the three-hundredth maximum of the spectrum, respectively.

bin of photogenerated carriers within the localized states at the band tails and are responsible for the shifts. After excitation, the electrons or holes lose their energy by thermalization at the band-tail states, which induces the PL redshift at an early stage.<sup>11</sup> The decay process at this stage will be discussed later.

The blueshift is generally observed in the middle time range.<sup>10,11,16,17</sup> If the upper and lower localized states involved in the recombination become charged, when they capture, respectively, an electron and a hole, and the Coulombic interaction energy will be lost on their return to neutral states through the electron-hole recombination. Assuming a tunneling process in the recombination, the PL lifetime becomes longer because the recombination probability decreases if the distance between the electron-hole pair is longer, while the Coulombic energy loss decreases. Hence, the PL shifts to a higher energy as the delay time increases.<sup>10,11,16,17</sup> Good examples of the blue shift can be found in  $a\text{-SiO}_x\text{:H}$  (Refs. 10 and 11) and  $a\text{-SiC}_x\text{:H}$  (Ref. 17). The carbon or oxygen incorporation in  $a\text{-Si:H}$  leads to a decrease in dielectric constant and an increase in the Coulombic energy of the electron-hole pair.<sup>10,11,17</sup> A similar phenomenon can be found in the present samples in which nitrogen is incorporated. As shown in Fig. 2, the blueshift is not pronounced in sample F, where the dielectric constant is the largest. The relationship in which the sample with a lower dielectric constant shows that a clearer blueshift was observed among all seven samples. This shows that the blueshift observed in the present  $a\text{-SiN}_x\text{:H}$  results from the Coulombic interaction.

The final redshift is attributed to the extent of localization of the carriers, which varies with the energy of the band-tail states. Electrons and holes in the deeper states are more localized, and this leads to a longer lifetime of the electron-hole pair in the frame of the radiative tunneling model.<sup>11</sup> As a result, the PL shifts to lower energies with time.

Figure 3(a) shows the changes in the total PL intensity as a function of time observed in samples A, B, and F. The PL decays are nonexponential, ranging from  $\sim 10^{-8}$  to  $10^{-3}$  s, which indicates that the PL has a broad lifetime distribution.

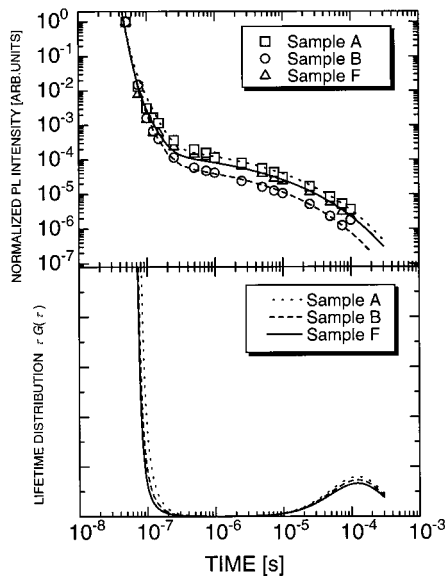


FIG. 3. (a) The PL decays and (b) lifetime distributions of samples A, B, and F measured over the time range of  $10^{-8}$ – $10^{-3}$  s using the excimer laser excitation at room temperature.

Therefore, it is convenient to analyze the PL decay by a distribution  $G(\tau)$  of lifetime  $\tau$ . The curves in Fig. 3(a) were drawn by choosing  $G(\tau)$  so as to yield the best fits to the decays according to the procedure suggested by Tsang and Street.<sup>12</sup> Figure 3(b) shows the product  $\tau G(\tau)$  or the lifetime distribution as calculated from Fig. 3(a). The lifetime distribution  $\tau G(\tau)$  shows a peak at  $\tau = 1.2 \times 10^{-4}$  s regardless of the sample. It has been reported that  $\alpha$ -Si:H (Ref. 12) and  $\alpha$ -SiC<sub>x</sub>:H (Refs. 17 and 18) have similar peaks at  $10^{-6}$ – $10^{-3}$  s, and radiative tunneling was suggested as the main recombination mechanism. This suggested mechanism is quite consistent with the above-noted explanation for the blueshift and the final redshift in PL in the present experiment.

In Fig. 3 a steep drop in  $\tau G(\tau)$  is seen at  $\tau \approx 10^{-7}$  s, the same time range wherein the initial redshift in the time-resolved spectra is observed. In order to study this further, the PL decay at this early stage was investigated using SR. Figure 4 shows nanosecond-order PL decay curves for sample B monitored at various emission energies. All of the measurements were performed at 20 K, and under excitation by SR photons with an energy of 5.0 eV. The decays are nonexponential and can be expressed by a stretched exponential function,

$$I(t) \propto (\tau'/t)^{1-\beta} \exp[-(t/\tau')^\beta], \quad (1)$$

where  $I$  is the PL intensity,  $t$  the time,  $\tau'$  the effective lifetime, and  $\beta$  a parameter that has a value between 0 and 1. The curves in Fig. 4 are the results of the least-squares fit of the decay profiles to Eq. (1). As the photon energy increases,  $\tau'$  becomes shorter while  $\beta$  stays almost constant at  $\sim 0.4$ . The average lifetime  $\tau_{\text{ave}}$  was obtained by assuming the stretched exponential to be composed of an infinite number of single exponentials with their distribution  $G(\tau)$ .<sup>19</sup> Figure 5 shows the calculated  $\tau_{\text{ave}}$  for each emission energy. A negative exponential dependence,  $\tau_{\text{ave}} \propto \exp(-E/\gamma)$ , on the emission energy  $E$  is seen, and the logarithmic slope  $\gamma$  was

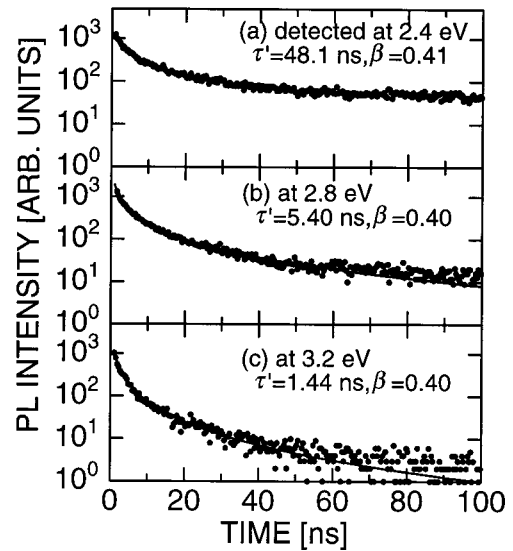


FIG. 4. The nanosecond-order decays of sample B monitored at various PL emission energies, (a) 2.4 eV, (b) 2.8 eV, and (c) 3.2 eV using SR excitation at 20 K. The curves are the best fits of the stretched-exponential function, Eq. (1).

determined to be 316 meV by the least-squares fit. This dependence is explained by a nonradiative hopping process of photogenerated carriers within the localized states at the band tails.<sup>19</sup> At low temperatures, the phonon-assisted hopping is a dominant process that decreases the population of carriers at a certain energy state together with radiative recombination.<sup>20</sup> Because the hopping rate is proportional to the density of states (DOS) and the DOS profile at band tails in  $\alpha$ -SiN<sub>x</sub>:H is exponential,<sup>21</sup> the average lifetime is expected to decrease exponentially with an increase in photon energy.<sup>19</sup>

A fast PL decay component ( $\tau < 10^{-8}$  s) at low temperatures around 15 K was also found in  $\alpha$ -SiC<sub>x</sub>:H.<sup>18</sup> Based on the fact that this component appears only in the samples with  $x > 0.25$ , acceleration of the radiative recombination rate by a

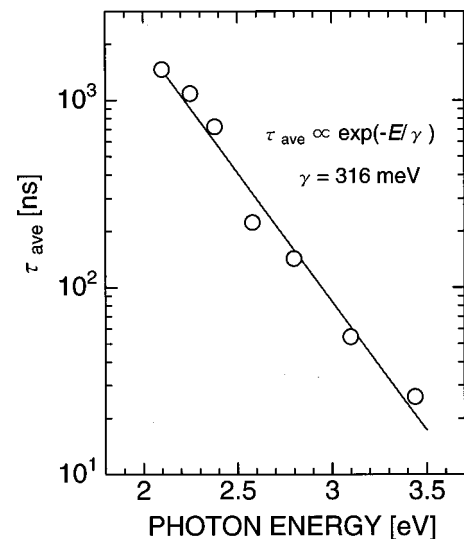


FIG. 5. The average lifetime of the nanosecond-order decay as a function of the emission energy. The solid line is the least-squares exponential fit to the data.

strong Coulombic interaction has been suggested as being responsible for this component.<sup>18</sup> The same logic can be applied to the present  $\alpha$ -SiN<sub>x</sub>:H, because the fast decay is commonly observed in  $\alpha$ -SiN<sub>x</sub>:H but is absent in  $\alpha$ -Si:H.<sup>5,11–15,19</sup> Therefore, recombination of an electron-hole pair bound by a strong Coulombic force, e.g., an exciton, is considered to be the radiative mechanism for the fast decay component. Continuing the discussion developed in relation to Fig. 2, the excitonlike electron-hole pairs are thermalized while they recombine with each other via the above-mentioned radiative process.

In summary, the time-resolved PL measurements on  $\alpha$ -SiN<sub>x</sub>:H indicate that the photogenerated carriers within the band-tail states recombine first through an excitonlike

mechanism and then through a radiative tunneling mechanism, leading to a broad lifetime distribution expanding from nanoseconds to milliseconds. Furthermore, contributions such as thermalization by the hopping process, the Coulombic interaction, and the extent of localization on the recombination process result in a time-evolved PL shift.

This work was partly supported by the 1998 Joint Studies Program of the UVSOR Facility, Institute for Molecular Science, Okazaki, Japan, and by a Grant-in-Aid (No. 09450132) from the Ministry of Education, Science, Sports, and Culture of Japan. One of the authors (M. F.) would like to thank the Japan Society for the Promotion of Science for financial support.

---

\*Email address: yohki@mn.waseda.ac.jp

<sup>1</sup>P. M. Lenahan, D. T. Krick, and J. Kanicki, *Appl. Surf. Sci.* **39**, 392 (1989).

<sup>2</sup>W. L. Warren, J. Kanicki, F. C. Rong, and E. H. Poindexter, *J. Electrochem. Soc.* **139**, 880 (1992).

<sup>3</sup>W. L. Warren, F. C. Rong, E. H. Poindexter, G. J. Gerardi, and J. Kanicki, *J. Appl. Phys.* **70**, 346 (1991).

<sup>4</sup>W. L. Warren, P. M. Lenahan, and J. Kanicki, *J. Appl. Phys.* **70**, 2220 (1991).

<sup>5</sup>K. S. Seol, T. Futami, T. Watanabe, Y. Ohki, and M. Takiyama, *J. Appl. Phys.* **85**, 6746 (1999).

<sup>6</sup>S. V. Deshpande, E. Gulari, S. W. Brown, and S. C. Rand, *J. Appl. Phys.* **77**, 6534 (1995).

<sup>7</sup>D. Chen, J. M. Viner, P. C. Taylor, and J. Kanicki, *J. Non-Cryst. Solids* **182**, 103 (1995).

<sup>8</sup>V. V. Vasilev, I. P. Mikhailovskii, and K. K. Svitashv, *Phys. Status Solidi A* **95**, K37 (1986).

<sup>9</sup>V. V. Vasilev and I. P. Mikhailovskii, *Phys. Status Solidi A* **90**,

355 (1985).

<sup>10</sup>R. A. Street, *Solid State Commun.* **34**, 157 (1980).

<sup>11</sup>R. A. Street, *Adv. Phys.* **30**, 593 (1981).

<sup>12</sup>C. Tsang and R. A. Street, *Phys. Rev. B* **19**, 3027 (1979).

<sup>13</sup>S. Kurita, W. Czaja, and S. Kinmond, *Solid State Commun.* **32**, 879 (1979).

<sup>14</sup>R. A. Wilson and T. P. Kerwin, *Phys. Rev. B* **25**, 5276 (1982).

<sup>15</sup>I. Hirabayashi, K. Morigaki, and S. Nitta, *J. Phys. Soc. Jpn.* **50**, 2961 (1981).

<sup>16</sup>R. W. Collins and W. Paul, *Phys. Rev. B* **25**, 2611 (1982).

<sup>17</sup>W. Siebert, R. Carius, W. Fuhs, and K. Jahn, *Phys. Status Solidi B* **140**, 311 (1987).

<sup>18</sup>L. R. Tessler, *Solid State Commun.* **111**, 193 (1999).

<sup>19</sup>F. Giorgis, C. F. Pirri, C. Vinegoni, and L. Pavesi, *Phys. Rev. B* **60**, 11 572 (1999).

<sup>20</sup>S. Kivelson and C. D. Gelatt, Jr., *Phys. Rev. B* **26**, 4646 (1982).

<sup>21</sup>J. Robertson, *Philos. Mag. B* **63**, 47 (1991).